JACS
JOURNAL OF THE AMERICAN CHEMICAL SOCIETY

pubs.acs.org/JACS

Article

Understanding the Structure−Polymerization Thermodynamics Relationships of Fused-Ring Cyclooctenes for Developing Chemically Recyclable Polymers

Junfeng Zhou, Devavrat Sathe, and Junpeng Wang*

Cite This: *J. Am. Chem. Soc.* 2022, 144, 928−934

Read Online

ACCESS | Metrics & More | Article Recommendations | Supporting Information

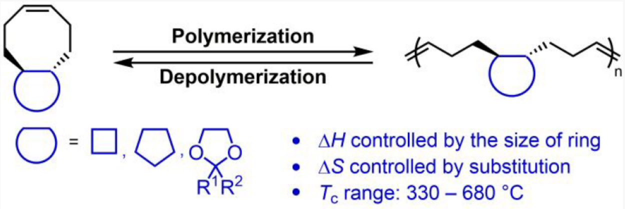

ABSTRACT: Polymers that can be chemically recycled to their constituent monomers offer a promising solution to address the challenges in plastics sustainability through a circular use of materials. The design and development of monomers for next-generation chemically recyclable polymers require an understanding of the relationships between the structure of the monomers/polymers and the thermodynamics of polymerization/depolymerization. Here we investigate the structure−polymerization thermodynamics relationships of a series of cyclooctene monomers that contain an additional ring fused at the 5,6-positions, including *trans*-cyclobutane, *trans*-cyclopentane, and *trans*-five-membered cyclic acetals. The four- and five-membered rings *trans*-fused to cyclooctene reduce the ring strain energies of the monomer, and the enthalpy changes of polymerizations are found to be in the range of -2.1 to -3.3 kcal mol^{-1}. Despite the narrow range of enthalpy changes, the ceiling temperatures at 1.0 M span from 330 to 680 °C, due to the low entropy changes, ranging from -2.7 to -5.0 cal mol^{-1} K^{-1}. Importantly, geminal substituents on the *trans*-five-membered cyclic acetal fused cyclooctenes are found to reduce the ceiling temperature by ∼300 °C, although they are not directly attached to the cyclooctene. The remote *gem*-disubstituent effect demonstrated here can be leveraged to promote depolymerization of the corresponding polymers and to tune their thermomechanical properties.

■ INTRODUCTION

Polymers have been used as indispensable materials in nearly every aspect of human activities, including clothing, packaging, construction, and transportation, owing to their light weight, chemical and thermal stability, flexibility, and processability. However, due to their durability, current polymer products are largely unrecycled after their service life, and the accumulation of these polymers has caused serious plastic pollution.[1−4] In addition, since most polymers are produced from finite fossil fuels, the lack of recycling has raised concerns regarding the sustainability of their use. Traditionally, a small fraction of plastic waste is subjected to physical or mechanical recycling where the plastics are ground into small particles for low-grade use.[5] In recent years, chemical recycling to monomers (CRM) has received increased attention as a promising strategy to address the challenges in plastics sustainability, as the recycled monomers can be repolymerized to form polymers with quality comparable to that of the virgin polymers.[6−8] The closed-loop recycling of plastics not only addresses the end-of-life accumulation issue but also allows the finite resources to be reused.

A suitable CRM system requires practical depolymerization conditions so that the recycling process is energy-efficient and does not lead to monomer decomposition. On the other hand, the polymer needs to be stable under its service conditions. To balance the stability and depolymerizability, the thermodynamics of polymerization/depolymerization need to be carefully controlled.[9,10] While exceptions exist, a polymerization reaction is typically characterized by a favorable enthalpy change ($\Delta H < 0$) and an unfavorable entropy change ($\Delta S < 0$); there exists a temperature, termed ceiling temperature (T_c), at which the two factors are canceled out.[11−13] Recently, CRM has been demonstrated with several systems that are based on cyclic monomers; the polymers can be formed through ring-opening polymerization of the cyclic monomers, and CRM can proceed through ring-closing depolymerization to form the cyclic monomers.[14−27] The success with cyclic monomers can be attributed to their milder enthalpy change in polymerization and therefore lower T_c compared to vinyl monomers. In addition, depolymerization of the polymers to their cyclic monomers typically requires catalysts; without the catalysts, the polymers are in a metastable equilibrium and can be stable above their T_cs.[15,22] Examples of CRM monomers include lactones,[14−18] thiolactones,[19−21,23] cyclic carbonates,[24,25] cyclic acetals,[22] and

Received: October 22, 2021
Published: January 5, 2022

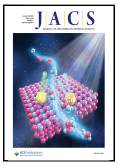

cycloalkenes.[26,27] Cycloalkene-based CRM systems are desirable, as they can access polymers with a hydrocarbon backbone, which have greater hydrolytic stability compared to other systems; however, cycloalkenes have been underexplored in the context of CRM. The demonstrated systems have been focused on five-membered cyclic olefins, including cyclopentene[26,28] or dihydrofuran,[27] but only polymers with glass transition temperatures (T_gs) below or near room temperature have been prepared from those monomers.[28] Recently, our group demonstrated that a *trans*-cyclobutane fused at the 5,6-positions of cyclooctene can reduce the ring strain energy (RSE) of cyclooctene to a level comparable to those of the five-membered cyclic olefins.[29] This reduction of RSE was found to be critical for CRM: Polymers formed from ring-opening metathesis polymerization (ROMP) of the *trans*-cyclobutane-fused cyclooctene (*t*CBCO) monomers can undergo depolymerization to form the monomers under mild conditions. In contrast, the ROMP polymer of the unsubstituted cyclooctene does not undergo depolymerization under identical conditions. In addition, the T_cs of *t*CBCO monomers are >160 °C higher than that of cyclopentene ($T_c \approx 30$ °C at 1.0 M)[30,31] due to a significantly lower entropy loss during polymerization. The favorable thermodynamics allows the preparation of polymers of high molecular weights with a variety of functional groups on cyclobutane; the thermomechanical properties of the polymers can thus be tuned, and both rubbery and plastic materials can be accessed.[29]

Encouraged by the potential of the fused-ring cyclooctene system in CRM, herein we explore the relationships between the monomer structure and the polymerization thermodynamics of the fused-ring cyclooctenes (Figure 1a), aiming to establish design principles that can be useful for developing CRM polymers. Guided by our previous calculations, which show that the RSE of a *trans*-cyclopentane-fused cyclooctene (5.3 kcal mol^{-1}) is close to that of *t*CBCO (**M1**, RSE = 4.9 kcal mol^{-1}), we extend the thermodynamic studies to the *trans*-cyclopentane-fused cyclooctene (**M2**, Figure 1b). In addition, replacing the cyclopentane in **M2** with a five-membered cyclic acetal leads to **M3**, which has an RSE of 5.1 kcal/mol (Table S1). The synthetic convenience of the acetal allows for **M3** with various functional groups to be accessed (**M3a**−**M3e**, Figure 1b). The substituent effects on the thermodynamics of polymerization and on the depolymerization of the corresponding polymers were systematically investigated. Importantly, reduced T_cs were observed for the monomers with geminal substituents—**M3c** and **M3d**—suggesting a remote Thorpe−Ingold effect.[32] The structure—thermodynamics relationships explored here can guide the future monomer design for CRM polymers.

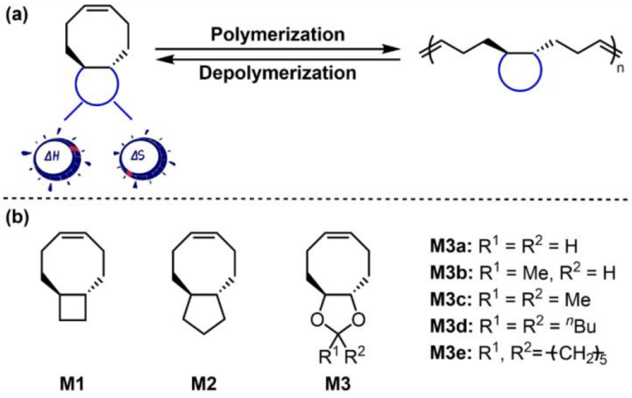

Figure 1. Tuning the polymerization thermodynamics of the fused-ring cyclooctene monomers. (a) Installing an appropriate ring on cyclooctene makes the corresponding ROMP polymer depolymerizable, and the enthalpy changes and entropy changes of polymerization can be tuned through the additional ring. (b) Monomers that are used for thermodynamic studies in this work.

■ RESULTS AND DISCUSSION

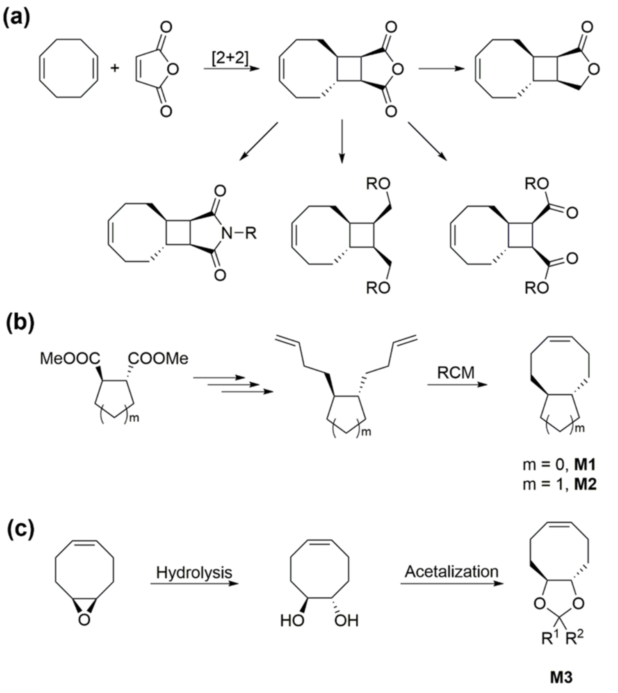

Figure 2. Syntheses of fused-ring cyclooctene monomers. (a) Synthetic scheme of *trans*-cyclobutane-fused cyclooctene monomers with substituents on the cyclobutane. (b) Synthetic scheme of the unsubstituted *trans*-cyclobutane-fused cyclooctene (**M1**) and *trans*-cyclopentane-fused cyclooctene (**M2**). (c) Synthetic scheme of the *trans*-five-membered cyclic acetal cyclooctene monomers (**M3**).

In our previous study (Figure 2a), *t*CBCO monomers with substituents on cyclobutane were prepared from the photochemical [2+2] cycloaddition adduct of 1,5-cyclooctadiene and maleic anhydride. Since both the fused-cyclobutane and the substituents are introduced, it is unclear how much each factor impacts the thermodynamics of polymerization and depolymerization. Herein, we set out to investigate the thermodynamics of the unsubstituted monomers **M1**, **M2**, and **M3a**. The syntheses of **M1** and **M2** are shown in Figure 2b. At first, the diester of *cis*-cyclobutane or *cis*-cyclopentane was refluxed in methanol under basic condition to form the corresponding *trans*-cycloalkane diester.[33,34] $LiAlH_4$ reduction converted the diester into the diol, which was subjected to tosylation followed by nucleophilic substitution with allylmagnesium bromide, affording the diene. RCM of the dienes of *trans*-cyclobutane and *trans*-cyclopentane affords **M1** and **M2**, respectively. **M3** can be synthesized through a one-step acetalization of *trans*-5,6-dihydroxy cyclooctene (Figure 2c), which, compared to the synthesis of **M1** and **M2**, is simpler and more suitable for scaling up. Since the substituent on **M3** can be conveniently varied by using different aldehydes/

https://doi.org/10.1021/jacs.1c11197
J. Am. Chem. Soc. 2022, 144, 928−934

ketones to react with *trans*-5,6-dihydroxy cyclooctene, **M3** serves as a convenient platform for investigating the substituent effects on the polymerization thermodynamics. Therefore, five *trans*-cyclic acetal fused cyclooctenes with different substituents, including **M3a**, **M3b**, **M3c**, **M3d**, and **M3e**, were prepared (Figure 1b).

Table 1. Molecular Weight Information and Thermal Properties of Polymers Prepared from Fused-Ring Cyclooctene Monomers[a]

Entry	Structure	M_n (kDa)[b]	$Đ$[c]	T_d (°C)[d]	T_g (°C)[e]
P1	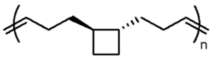	58	1.61	391	-55
P1$_{ester}$[f]	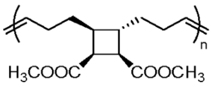	142	1.55	401	18
P1$_{ether}$[f]	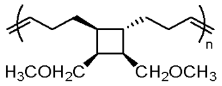	293	1.91	372	-34
P1$_{imide}$[f]	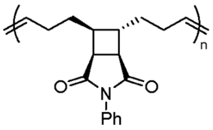	198	1.96	409	100
P2	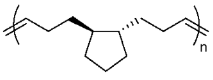	82	1.64	405	-33
P3a	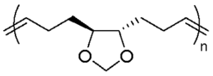	171	1.71	360	-30
P3b	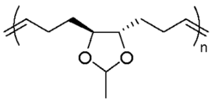	102	1.78	367	-14
P3c	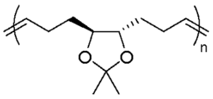	247	1.89	342	-4
P3d	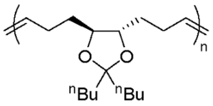	164	2.08	327	-27
P3e	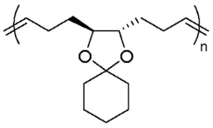	258	1.86	347	8

[a]All polymerizations were conducted under ambient conditions in dichloromethane with Grubbs 2nd-generation catalyst as the initiator. [b]M_n, number-average molecular weight, determined by gel permeation chromatography (GPC) in THF using a standard molecular weight method. [c]$Đ$, dispersity, M_w/M_n, determined by GPC. [d]T_d, decomposition temperature, defined as the temperature at which 5% weight loss occurs, measured by thermogravimetric analysis. [e]T_g, glass transition temperature, measured by differential scanning calorimetry. [f]Molecular weight information and thermal properties of these polymers were reported in ref 29.

Each monomer was subjected to ROMP with Grubbs second-generation catalyst (**G2**) as the initiator under ambient conditions overnight. The polymerization was conducted in dichloromethane at an initial monomer concentration of 2.0 M and a monomer to initiator ratio of 500:1 or 1000:1. The resulting molecular weight information and thermal properties were collected and summarized in Table 1. Polymers of high molecular weights (>50 kDa) were obtained in all cases; the dispersity ($Đ$) values were found to range from 1.6 to 2.1. The polymers show high thermal stability, with decomposition onset temperatures (T_d, defined as the temperature at which a sample experiences 5% weight loss) above 320 °C. The glass transition temperatures (T_g) range from −55 to 8 °C.

Having the T_g of the unsubstituted *t*CBCO polymer **P1** (−55 °C) measured allows us to assess the substituent effects on glass transition. For example, according to our recent work, when the two hydrogens on cyclobutane are replaced with two methyl esters (**P1$_{ester}$**), two methyl ethers (**P1$_{ether}$**), or an imide fused ring (**P1$_{imide}$**), the T_gs of the corresponding polymers were found to be 18, −34, and 100 °C, respectively. From **P1** to **P2**, as the cyclobutane is replaced with a cyclopentane, the T_g increases from −55 °C to −33 °C. Replacement of the cyclopentane in **P2** with a five-membered acetal (**P3a**, T_g = −30 °C) was found not to significantly alter the glass transition temperature. In addition, compared to the unsubstituted polymer **P3a**, the T_gs of the monomethyl (**P3b**) and *gem*-dimethyl (**P3c**) substituted polymers were found to be −14 and −4 °C, respectively. Replacing the two methyl groups in **P3c** with two *n*-butyl groups in **P3d** leads to a decreased T_g from −4 °C to −27 °C. In addition, replacing the two hydrogens in **P3a** with a cyclohexane ring leads to a spiro ketal polymer (**P5e**) with a T_g of 8 °C.

To investigate the thermodynamics of polymerization, the polymerization was conducted at various temperatures ranging from room temperature to 65 °C, at an initial monomer concentration of 1.0 M in xylenes with 1 mol % of **G2**. The polymerization was allowed to proceed for 6 h, which according to the kinetic studies (Figure 3), is sufficient for the system to reach an equilibrium. The concentration of the remaining monomer at equilibrium $[M]_e$ was characterized by ^{1}H NMR and listed in Table 2. The logarithm of $[M]_e$ was plotted against the inverse of temperature, and the plot was fit to eq 1, allowing for both ΔH and ΔS of the polymerization to be extracted (Table 3).

$$\ln[M]_e = \frac{\Delta H}{RT} - \frac{\Delta S}{R} \qquad (1)$$

The ΔH values for **M1**, **M2**, and **M3** (including **M3a−M3e**) are all in the range of −2.1 to −3.3 kcal mol^{-1}, while the ΔS values are in the range of −2.7 to −5.0 cal mol^{-1} K^{-1}. Note that the ΔH values are lower than the RSEs obtained from DFT calculations (Table S1). This difference can be attributed to the presence of macrocyclic oligomers during the thermodynamic studies of polymerization,[29] whereas the calculation of RSEs does not take into account those structures (see SI for details). Despite the narrow range in both ΔH and ΔS, the resulting ceiling temperatures T_c at 1.0 M differ by a span of 340 °C, which can be attributed to the low absolute values of ΔH and ΔS. For example, although there is only a difference of 0.8 kcal mol^{-1} between the ΔH of **M1** and **M2**, this difference corresponds to 38% in ΔH of **M1** (−2.1 kcal mol^{-1}). In fact, the 45% increase in T_c from **M1** (335 °C) to **M2** (614 °C) is mainly due to the enhanced ΔH, as the $\Delta\Delta S$ between the two monomers—0.2 kcal mol^{-1}—is only ~6% in the ΔS of **M1**. These results show that from **M1** to **M2**, as the ring fused to cyclooctene changed from cyclobutane to cyclopentane, the effects on thermodynamics are primarily

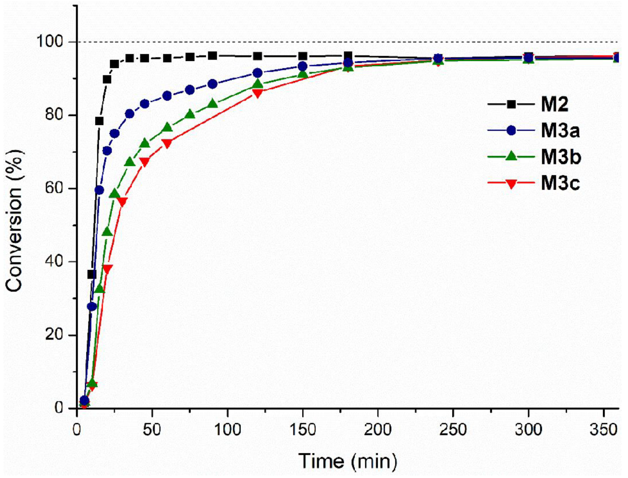

Figure 3. Kinetic studies of polymerization. Conversion of polymerization is plotted against polymerization time for **M2**, **M3a**, **M3b**, and **M3c**. Each polymerization was conducted at an initial monomer concentration of 1.0 M under ambient conditions, with Grubbs 2nd-generation catalyst as the initiator.

enthalpic. From **M2** to **M3a**, as cyclopentane is replaced with cyclic acetal, no significant change was observed in Δ*H*, Δ*S*, or T_c.

The higher ceiling temperatures of **M2** and **M3a**, compared to that of **M1**, were also reflected in their depolymerization behaviors. After the polymer solutions (in $CDCl_3$, [olefin] = 25 mM) were stirred with 1 mol % **G2** catalyst at 50 °C for 2 h, the resulting solutions were characterized by ^1H NMR spectra. It was found that while **P2** and **P3a** still showed visible oligomer peaks in the range of 5.5−5.3 ppm, those peaks were absent for **P1** (Figure 4). Integration of ^1H NMR peaks showed that the percentages of formation of **M1**, **M2**, and **M3a** are 98%, 84%, and 91%, respectively. In addition, the favorable thermodynamics in forming **M1** over **M2** was also shown in their synthesis through the ring-closing metathesis (RCM) of their diene precursors (Figure S28): While the *trans*-cyclobutane diene can be quantitatively converted into **M1**, RCM of the *trans*-cyclopentane diene resulted in a mixture of **M2** and some side products.

Table 3. Polymerization Thermodynamic Data for Fused-Ring Cyclooctene Monomers

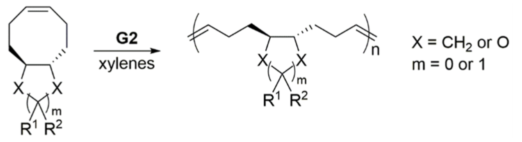

Entry	Structure	Δ*H* (kcal mol^{-1})	Δ*S* (cal mol^{-1} K^{-1})	T_c at 1.0 M (°C)
M1	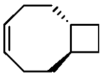	-2.1 ± 0.1	-3.4 ± 0.3	335
M1$_{ester}$[a]	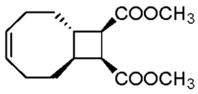	-1.7 ± 0.3	-3.6 ± 0.9	199
M1$_{imide}$[a]	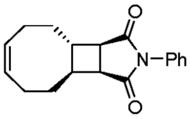	-2.8 ± 0.5	-4.9 ± 1.6	295
M2	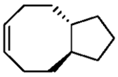	-2.9 ± 0.3	-3.2 ± 0.8	614
M3a	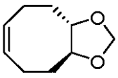	-2.7 ± 0.2	-2.9 ± 0.7	646
M3b	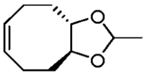	-2.6 ± 0.2	-2.7 ± 0.7	675
M3c	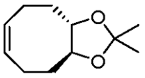	-3.2 ± 0.1	-4.9 ± 0.3	376
M3d	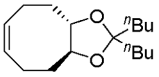	-3.3 ± 0.2	-5.0 ± 0.6	380
M3e	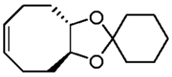	-2.8 ± 0.1	-3.3 ± 0.5	571

[a] The polymerization thermodynamic data for these monomers were reported in ref 29.

Because of the facile synthesis and functionalization of **M3**, we explored the substituent effects on the polymerization and depolymerization in order to bring its thermodynamics closer to that of **M1**. Compared to **M3a** (T_c = 646 °C), the introduction of a methyl substituent in **M3b** (T_c = 675 °C) did not significantly alter the T_c. However, when another methyl group was added in **M3c**, the T_c was reduced to 376 °C. Changing the two methyl groups in **M3c** into two *n*-butyl groups in **M3d**, the T_c (= 380 °C) was not significantly altered. In addition, when the geminal methyl groups or *n*-butyl groups were replaced with a cyclohexane in **M3e**, the T_c went back to 571 °C. These results indicate a *gem*-disubstituent effect that reduces the ceiling temperature of polymerization and favors depolymerization of the corresponding polymers. It has been well documented that the *gem*-disubstituent effect, also termed

Table 2. Average of Monomer Concentration at Equilibrium $[M]_e$ (mol/L) for All Monomers at Different Temperatures[a]

	rt	35 °C	45 °C	55 °C	65 °C
M1	0.156 ± 0.002	0.183 ± 0.003	0.212 ± 0.003	0.229 ± 0.002	0.257 ± 0.005
M2	0.037 ± 0.001	0.046 ± 0.002	0.053 ± 0.001	0.065 ± 0.001	0.074 ± 0.003
M3a	0.042 ± 0.001	0.052 ± 0.001	0.065 ± 0.000	0.070 ± 0.001	0.078 ± 0.002
M3b	0.047 ± 0.001	0.055 ± 0.001	0.063 ± 0.003	0.076 ± 0.001	0.086 ± 0.002
M3c	0.047 ± 0.001	0.063 ± 0.001	0.078 ± 0.001	0.087 ± 0.001	0.101 ± 0.001
M3d	0.047 ± 0.001	0.060 ± 0.002	0.070 ± 0.001	0.081 ± 0.005	0.101 ± 0.003
M3e	0.044 ± 0.003	0.056 ± 0.001	0.063 ± 0.002	0.071 ± 0.002	0.086 ± 0.002

[a] The initial monomer concentration $[M]_0$ is 1.0 M.

https://doi.org/10.1021/jacs.1c11197
J. Am. Chem. Soc. 2022, 144, 928−934

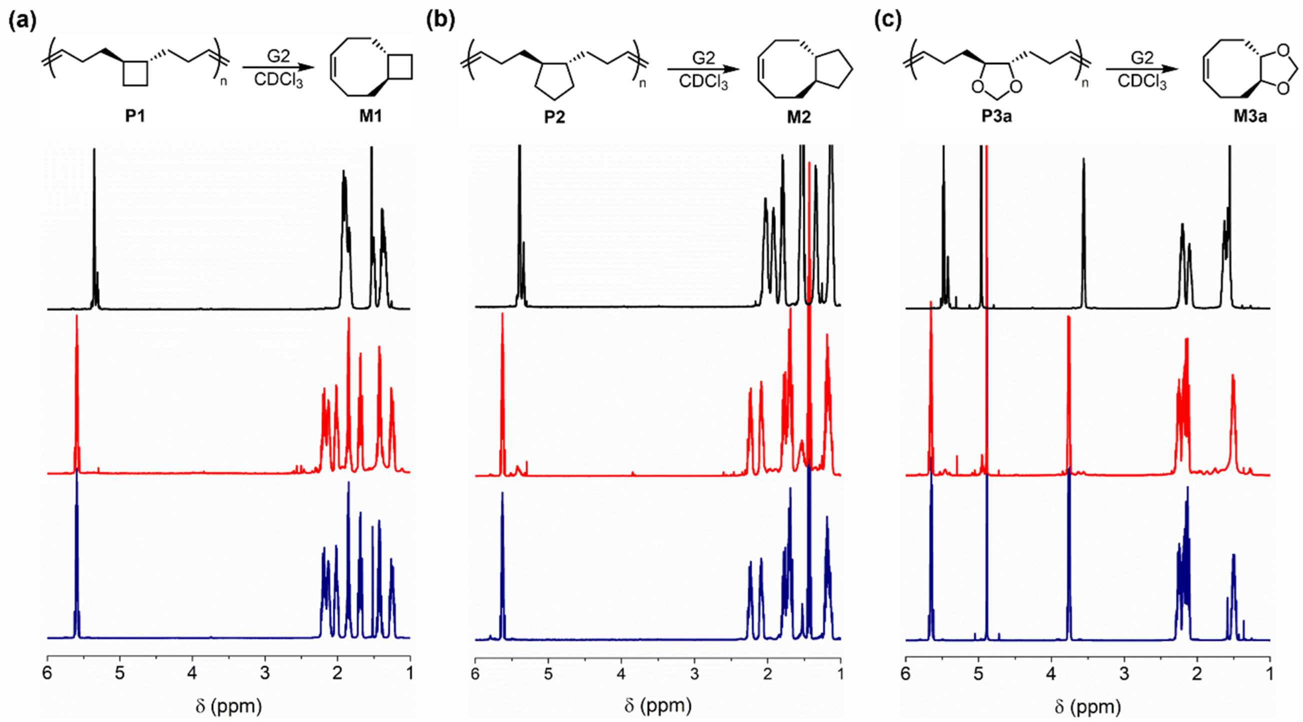

Figure 4. Depolymerization of the fused-ring cyclooctene polymers. The ^{1}H NMR spectra for **P1** (a), **P2** (b), and **P3a** (c) before (in black) and after (in red) heating at 50 °C for 2 h in the presence of 1 mol % Grubbs 2nd-generation catalyst. The ^{1}H NMR spectrum for each monomer was also shown as the reference (in blue). Oligomer peaks in the range of 5.5−5.3 ppm were observed for the depolymerization of **P2** and **P3a**, but not for **P1**, indicating more favorable thermodynamics of depolymerization for **P1**.

as the Thorpe−Ingold effect, can promote cyclization reactions;[21,32,35−38] yet the finding here is distinct in that the geminal substituents and the cyclooctene are not directly linked but are rather separated by a cyclic acetal.

The remote geminal substituents in **M3c** and **M3d** were found to result in more negative ΔH and ΔS, which correspond to increased and decreased T_c, respectively. The observed ∼300 °C reduction in T_c means the entropic effect overrides the enthalpic one, leading to a net decrease in T_c. The entropy change in polymerization can be dissected into translational entropy change ΔS_t and rotational entropy change ΔS_r to facilitate the interpretation of the relationships.[39] The translational entropy change ΔS_t is negative for a polymerization as the more mobile monomers are connected to form the less mobile polymer; the magnitude of ΔS_t is largely determined by the molar mass and concentration of the monomer. In this case, the geminal substituents should not lead to a more negative ΔS_t, as they would only make the monomer less mobile, which corresponds to a less negative ΔS_t. This means the more negative ΔS resulting from the *gem*-disubstituent effect is mainly in ΔS_r. Since a ring-opening polymerization is positive in ΔS_r as it frees up the rotation of bonds, the reduced ΔS_r indicates less rotational freedom is gained in the *gem*-disubstituted systems. In other words, despite being remote, the geminal substituents still constrain the conformation of the polymer to an extent, resulting in a more negative entropy change for polymerization and a lower ceiling temperature. We note that T_cs at 1.0 M for **M3c** and **M3d** are 376 and 380 °C, respectively, close to that of **M1** (T_c = 335 °C). In addition, the remote *gem*-disubstituent effect was found to also impact kinetics of polymerization, as **M3c** showed the lowest polymerization rate (Figure 3). The fact that both thermodynamics and kinetics are tied with the remote *gem*-disubstituent effect resembles the regular Thorpe−Ingold effect, which has been shown to impact both aspects.[32]

To evaluate the remote *gem*-disubstituent effect on depolymerization, **P3a**−**P3e** solutions of various olefin concentrations, including 25, 50, 100, 200, and 400 mM, were stirred in the presence of 1 mol % **G2** at 50 °C for 2 h (Figure 5). For all polymers, the increased initial olefin concentrations led to the decrease in the formation of monomers, which is expected as the raised concentration

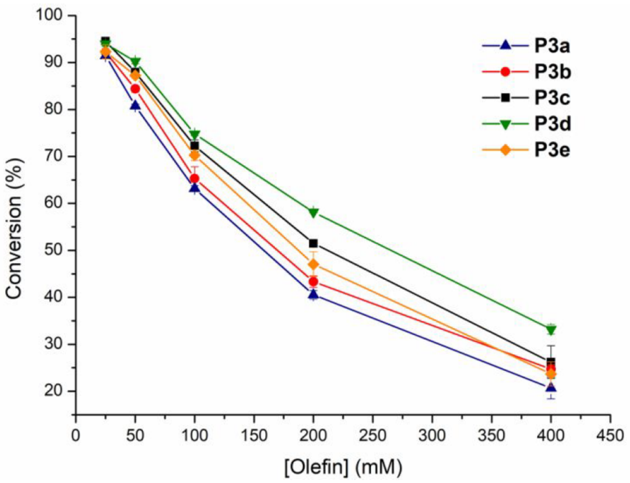

Figure 5. Depolymerization of **P3** at various olefin concentrations. The conversion of depolymerization, i.e., the percentage of monomer in the mixture, is plotted against the concentration of the initial concentration of the olefins in the polymer for each polymer. Each depolymerization was conducted in $CDCl_3$ at 50 °C for 2 h.

leads to reduced translational entropy gain to overcome the enthalpy penalty during depolymerization. Meanwhile, **P3c** and **P3d** were found to show higher percentages of depolymerization than the ones without the geminal substituents at all concentrations, and the gap between the *gem*-disubstituted and other polymers (i.e., **P3a**, **P3b**, and **P3e**) was more pronounced at high concentrations. For example, at the concentration of [olefin] = 25 mM, the percentages of depolymerization were all in the range of 90−95%; when the concentration was increased to [olefin] = 200 mM, both **P3c** and **P3d** showed percentages of depolymerization over 50%, whereas the values for **P3a** and **P3b** were ∼40%. The larger gap in percentage of depolymerization between the *gem*-disubstituted polymers and others at a higher concentration can be attributed to the decreased translational entropy gain and consequently the increased contribution from rotational entropy, which is impacted by the remote *gem*-disubstituent effect.

■ CONCLUSION

CRM polymers have shown the prospect for addressing the challenges in plastics sustainability through circular use of materials. Identifying the right monomers for CRM polymers that can replace current polymers is a key; the criteria include favorable thermodynamics for depolymerization as well as the tunable thermomechanical properties that can meet the needs for various applications. The fused-ring cyclooctene system provides rich opportunities to tune both thermodynamics and thermomechanical properties. Importantly, the enthalpic and entropic factors can be tuned independently, through the size of rings fused to cyclooctene and the substituents, respectively, resulting in a >300 °C span in ceiling temperatures. It should be noted that the absolute values of both enthalpy and entropy changes in this system are low—which is unique compared to other CRM systems—leading to highly sensitive structural effects on ceiling temperatures. As a result, geminal substituents, although not directly attached to cyclooctene, are found to significantly reduce the ceiling temperatures and promote depolymerization. The structure−thermodynamics relationships learned here provide insights into the design of monomers for CRM polymers.

Compared to the *t*CBCO monomers, the preparation of which requires a photochemical [2+2] cycloaddition reaction that is challenging to scale up, the facile synthesis of the *trans*-cyclic acetal-fused cyclooctene (*t*CACO) monomers makes them attractive for developing CRM polymers. This argument is further supported by the fact that the remote *gem*-disubstituent effect can help to bring the thermodynamics of the *t*CACO monomers close to that of *t*CBCO monomers. In addition, the geminal substituents in *t*CACO can be conveniently varied by using different ketones to prepare the ketals, allowing for the thermomechanical properties of the polymers to be tuned to meet the needs of various applications.

■ ASSOCIATED CONTENT

Supporting Information

The Supporting Information is available free of charge at https://pubs.acs.org/doi/10.1021/jacs.1c11197.

> Synthetic procedures, ring strain energies of the monomers, polymerization studies, depolymerization studies, NMR spectra, TGA and DSC curves, GPC traces, optimized geometries (PDF)

■ AUTHOR INFORMATION

Corresponding Author

Junpeng Wang − *School of Polymer Science and Polymer Engineering, The University of Akron, Akron, Ohio 44325, United States*; orcid.org/0000-0002-4503-5026; Email: jwang6@uakron.edu

Authors

Junfeng Zhou − *School of Polymer Science and Polymer Engineering, The University of Akron, Akron, Ohio 44325, United States*; orcid.org/0000-0002-8201-6799

Devavrat Sathe − *School of Polymer Science and Polymer Engineering, The University of Akron, Akron, Ohio 44325, United States*

Complete contact information is available at: https://pubs.acs.org/10.1021/jacs.1c11197

Notes

The authors declare no competing financial interest.

■ ACKNOWLEDGMENTS

This material is based upon work supported by University of Akron and the National Science Foundation under Grant No. 2042494. The computational resource was provided by the Extreme Science and Engineering Discovery Environment (TG-CHE190099).

■ REFERENCES

(1) Geyer, R.; Jambeck, J. R.; Law, K. L. Production, use, and fate of all plastics ever made. *Sci. Adv.* **2017**, *3*, e1700782.

(2) Fagnani, D. E.; Tami, J. L.; Copley, G.; Clemons, M. N.; Getzler, Y. D. Y. L.; McNeil, A. J. 100th anniversary of macromolecular science viewpoint: Redefining sustainable polymers. *ACS Macro Lett.* **2021**, *10* (1), 41−53.

(3) Millican, J. M.; Agarwal, S. Plastic pollution: A material problem? *Macromolecules* **2021**, *54* (10), 4455−4469.

(4) Hong, M.; Chen, E. Y. X. Future directions for sustainable polymers. *Trends Chem.* **2019**, *1* (2), 148−151.

(5) Schyns, Z. O. G.; Shaver, M. P. Mechanical recycling of packaging plastics: A review. *Macromol. Rapid Commun.* **2021**, *42* (3), e2000415.

(6) Closing the plastics loop. *Nature Sustainability* **2018**, *1* (5), 205−205.

(7) Coates, G. W.; Getzler, Y. D. Y. L. Chemical recycling to monomer for an ideal, circular polymer economy. *Nat. Rev. Mater.* **2020**, *5* (7), 501−516.

(8) Worch, J. C.; Dove, A. P. 100th anniversary of macromolecular science viewpoint: Toward catalytic chemical recycling of waste (and future) plastics. *ACS Macro Lett.* **2020**, *9* (11), 1494−1506.

(9) Olsen, P.; Odelius, K.; Albertsson, A. C. Thermodynamic presynthetic considerations for ring-opening polymerization. *Biomacromolecules* **2016**, *17* (3), 699−709.

(10) Schneiderman, D. K.; Hillmyer, M. A. Aliphatic polyester block polymer design. *Macromolecules* **2016**, *49* (7), 2419−2428.

(11) Höcker, H. Thermodynamic recycling—on ring-opening polymerization and ring-closing depolymerization. *J. Macromol. Sci., Part A: Pure Appl.Chem.* **1993**, *30* (9−10), 595−601.

(12) Cederholm, L.; Olsén, P.; Hakkarainen, M.; Odelius, K. Turning natural δ-lactones to thermodynamically stable polymers with triggered recyclability. *Polym. Chem.* **2020**, *11* (30), 4883−4894.

(13) Delgove, M. A. F.; Wróblewska, A. A.; Stouten, J.; van Slagmaat, C. A. M. R.; Noordijk, J.; De Wildeman, S. M. A.; Bernaerts, K. V. Organocatalyzed ring opening polymerization of regio-isomeric lactones: Reactivity and thermodynamics considerations. *Polym. Chem.* **2020**, *11* (21), 3573−3584.

(14) Hong, M.; Chen, E. Y. Completely recyclable biopolymers with linear and cyclic topologies via ring-opening polymerization of gamma-butyrolactone. *Nat. Chem.* **2016**, *8* (1), 42−9.

(15) Zhu, J.-B.; Watson, E. M.; Tang, J.; Chen, E. Y.-X. A synthetic polymer system with repeatable chemical recyclability. *Science* **2018**, *360*, 398−403.

(16) Shi, C.; Li, Z.-C.; Caporaso, L.; Cavallo, L.; Falivene, L.; Chen, E. Y. X. Hybrid monomer design for unifying conflicting polymerizability, recyclability, and performance properties. *Chem.* **2021**, *7* (3), 670−685.

(17) Li, L.-G.; Wang, Q.-Y.; Zheng, Q.-Y.; Du, F.-S.; Li, Z.-C. Tough and thermally recyclable semiaromatic polyesters by ring-opening polymerization of benzo-thia-caprolactones. *Macromolecules* **2021**, *54* (14), 6745−6752.

(18) Li, Y.-T.; Yu, H.-Y.; Li, W.-B.; Liu, Y.; Lu, X.-B. Recyclable polyhydroxyalkanoates via a regioselective ring-opening polymerization of *α,β*-disubstituted *β*-lactone monomers. *Macromolecules* **2021**, *54* (10), 4641−4648.

(19) Yuan, J.; Xiong, W.; Zhou, X.; Zhang, Y.; Shi, D.; Li, Z.; Lu, H. 4-hydroxyproline-derived sustainable polythioesters: Controlled ring-opening polymerization, complete recyclability, and facile functionalization. *J. Am. Chem. Soc.* **2019**, *141* (12), 4928−4935.

(20) Shi, C.; McGraw, M. L.; Li, Z.-C.; Cavallo, L.; Falivene, L.; Chen, E. Y.-X. High-performance pan-tactic polythioesters with intrinsic crystallinity and chemical recyclability. *Sci. Adv.* **2020**, *6*, eabc0495.

(21) Xiong, W.; Chang, W.; Shi, D.; Yang, L.; Tian, Z.; Wang, H.; Zhang, Z.; Zhou, X.; Chen, E.-Q.; Lu, H. Geminal dimethyl substitution enables controlled polymerization of penicillamine-derived *β*-thiolactones and reversed depolymerization. *Chem.* **2020**, *6* (7), 1831−1843.

(22) Abel, B. A.; Snyder, R. L.; Coates, G. W. Chemically recyclable thermoplastics from reversible-deactivation polymerization of cyclic acetals. *Science* **2021**, *373*, 783−789.

(23) Wang, Y.; Li, M.; Chen, J.; Tao, Y.; Wang, X. O-to-s substitution enables dovetailing conflicting cyclizability, polymerizability, and recyclability: Dithiolactone vs. Dilactone. *Angew. Chem., Int. Ed.* **2021**, *60* (41), 22547−22553.

(24) Liu, Y.; Zhou, H.; Guo, J. Z.; Ren, W. M.; Lu, X. B. Completely recyclable monomers and polycarbonate: Approach to sustainable polymers. *Angew. Chem., Int. Ed.* **2017**, *56* (17), 4862−4866.

(25) Saxon, D. J.; Gormong, E. A.; Shah, V. M.; Reineke, T. M. Rapid synthesis of chemically recyclable polycarbonates from renewable feedstocks. *ACS Macro Lett.* **2021**, *10* (1), 98−103.

(26) Neary, W. J.; Isais, T. A.; Kennemur, J. G. Depolymerization of bottlebrush polypentenamers and their macromolecular metamorphosis. *J. Am. Chem. Soc.* **2019**, *141* (36), 14220−14229.

(27) Feist, J. D.; Xia, Y. Enol ethers are effective monomers for ring-opening metathesis polymerization: Synthesis of degradable and depolymerizable poly(2,3-dihydrofuran). *J. Am. Chem. Soc.* **2020**, *142* (3), 1186−1189.

(28) Neary, W. J.; Kennemur, J. G. Polypentenamer renaissance: Challenges and opportunities. *ACS Macro Lett.* **2019**, *8* (1), 46−56.

(29) Sathe, D.; Zhou, J.; Chen, H.; Su, H.-W.; Xie, W.; Hsu, T.-G.; Schrage, B. R.; Smith, T.; Ziegler, C. J.; Wang, J. Olefin metathesis−based chemically recyclable polymers enabled by fused-ring monomers. *Nat. Chem.* **2021**, *13* (8), 743−750.

(30) Tuba, R.; Grubbs, R. H. Ruthenium catalyzed equilibrium ring-opening metathesis polymerization of cyclopentene. *Polym. Chem.* **2013**, *4* (14), 3959−3962.

(31) Liu, H.; Nelson, A. Z.; Ren, Y.; Yang, K.; Ewoldt, R. H.; Moore, J. S. Dynamic remodeling of covalent networks via ring-opening metathesis polymerization. *ACS Macro Lett.* **2018**, *7* (8), 933−937.

(32) Jung, M. E.; Piizzi, G. Gem-disubstituent effect: Theoretical basis and synthetic applications. *Chem. Rev.* **2005**, *105* (5), 1735−1766.

(33) Kean, Z. S.; Niu, Z.; Hewage, G. B.; Rheingold, A. L.; Craig, S. L. Stress-responsive polymers containing cyclobutane core mechanophores: Reactivity and mechanistic insights. *J. Am. Chem. Soc.* **2013**, *135* (36), 13598−604.

(34) Barton, L. M.; Edwards, J. T.; Johnson, E. C.; Bukowski, E. J.; Sausa, R. C.; Byrd, E. F. C.; Orlicki, J. A.; Sabatini, J. J.; Baran, P. S. Impact of stereo- and regiochemistry on energetic materials. *J. Am. Chem. Soc.* **2019**, *141* (32), 12531−12535.

(35) Forbes, M. D. E.; Patton, J. T.; Myers, T. L.; Maynard, H. D.; Smith, D. W.; Schulz, G. R.; Wagener, K. B. Solvent-free cyclization of linear dienes using olefin metathesis and the thorpe-ingold effect. *J. Am. Chem. Soc.* **1992**, *114* (27), 10978−10980.

(36) Kubota, H.; Yoshida, S.; Ouchi, M. Ring-expansion cationic cyclopolymerization for the construction of cyclic cyclopolymers. *Polym. Chem.* **2020**, *11* (24), 3964−3971.

(37) Wolf, W. J.; Li, J.; Jones, S. C.; Stoltz, B. M.; Grubbs, R. H. Efficient synthesis of geminal-dialkyl dienes for olefin metathesis polymerization. *Macromolecules* **2020**, *53* (18), 7803−7809.

(38) Park, H.; Lee, H.-K.; Choi, T.-L. Faster cyclopolymerisation of 4,4-disubstituted 1,7-octadiynes through an enhanced thorpe−ingold effect. *Polym. Chem.* **2013**, *4* (17), 46764681.

(39) Dainton, F. S.; Devlin, T. R. E.; Small, P. A. The thermodynamics of polymerization of cyclic compounds by ring opening. *Trans. Faraday Soc.* **1955**, *51* (0), 1710−1720.